Available online at www.sciencedirect.com

ScienceDirect

IFAC Papers Online CONFERENCE PAPER ARCHIVE

IFAC PapersOnLine 55-7 (2022) 470–476

Hierarchical nonlinear model predictive control of offshore hybrid power systems ⋆

Kiet Tuan Hoang * **Brage Rugstad Knudsen** **
Lars Struen Imsland *

* *Department of Engineering Cybernetics, Norwegian University of Science and Technology, Trondheim, Norway. E-mail: kiet.t.hoang@ntnu.no, lars.imsland@ntnu.no*

** *SINTEF Energy Research, Trondheim, Norway. E-mail: brage.knudsen@sintef.no*

Abstract: This paper presents an approach for controlling offshore hybrid power systems consisting of gas turbines, offshore wind, and batteries for satisfying an exogenous power demand. A hierarchical controller is developed comprising a high-level economic nonlinear model predictive controller that distributes the power demand according to some economic objective, a low-level nonlinear tracking model predictive controller that actuates on the hybrid power system, and a nonlinear moving horizon estimator to estimate the system state. Simulation results and concluding remarks reveal the advantage of such a hierarchical approach for a simple simulation study.

Keywords: Hierarchical control, Nonlinear predictive control, Industrial applications of optimal control, Power systems, Control of renewable energy resources.

1. INTRODUCTION

The offshore greenhouse gas (GHG) emissions account for a quarter of the total GHG emissions in Norway. To reduce GHG emissions, a reduction in offshore gas turbines as the primary power source is essential, as gas turbines account for most of the emissions offshore. One way of reducing the use of gas turbines is with the integration of renewable wind energy with batteries, see Fig. 1. (Norwegian Petroleum Directorate, 2019)

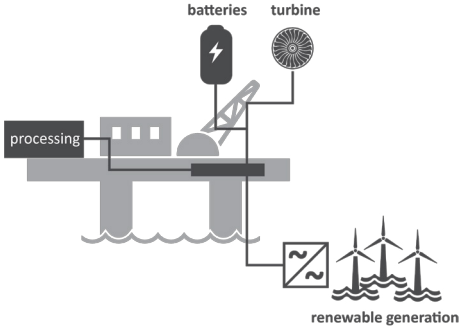

Fig. 1. Illustration of an offshore hybrid power system with wind energy and batteries, courtesy of SINTEF.

These offshore hybrid power systems (OHPSs) do not yet exist but can, in the future, offer the means to decarbonise the Norwegian Continental Shelf (NCS) energy infrastructure. They can, for example, be used as general offshore energy hubs (OEHs) for maritime transport, aquaculture, or green hydrogen production (Mikkola et al., 2018, Gea Bermúdez et al., 2021).

A suitable control methodology for constrained control of the resulting hybrid power system can be found in model predictive control (MPC). The MPC approach offers the advantage of considering the optimal inputs at the current time while also accounting for future optimal control inputs. Additionally, MPC can be extended for nonlinear systems like OHPSs (Rawlings et al., 2017).

Notably, economic model predictive control (EMPC) has shown success in similar applications as it can control and distribute power between different power systems according to some economic objective functions, see Hovgaard et al. (2010), Morstyn et al. (2018), or Kong et al. (2019). EMPC expands on the nominal MPC scheme with an economic control objective (Rawlings et al., 2012).

However, a notable disadvantage of an economic nonlinear model predictive control (ENMPC) scheme is the high computational cost associated with nonlinear systems and the long prediction horizons needed for taking advantage of future information. An example specific to the OHPS is future wind or exogenous power demand predictions. Computational delay may affect the control performance and stability of systems with strong nonlinearities and fast dynamics, see Findeisen and Allgöwer (2004).

To address the computational cost, process systems commonly employ a real-time optimiser (RTO) as a high-level controller (HLC), which computes optimal references in a hierarchical control structure with a fast low-level controller (LLC) for tracking and disturbance rejection, see Marlin and Hrymak (1997). An RTO can, however, only capture steady-state dynamics. Thus, extensions of an RTO that capture transient dynamics have been devel-

⋆ The Research Council of Norway funds this research through PETROSENTER LowEmission (project code 296207).

10.1016/j.ifacol.2022.07.488

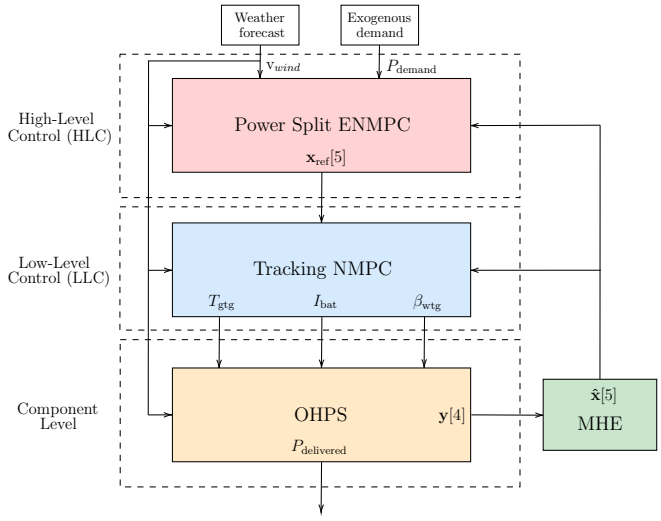

Fig. 2. An illustration of the hierarchical control strategy.

oped, for example, Würth et al. (2011), where the optimiser is a nonlinear model predictive controller (NMPC).

This paper investigates a hierarchical approach for plantwide optimisation and control of OHPSs consisting of offshore wind, gas turbines, and batteries. The approach uses an HLC-ENMPC to distribute the power load from arbitrarily power consumers, an LLC-NMPC for tracking the HLC references, and a moving horizon estimator (Kühl et al., 2011) to estimate the system states, see Fig. 2.

The main novelty of this study is the application of hierarchical ENMPC for coordinating the constrained power systems in an OHPS. Given future exogenous power demand and wind forecast knowledge, the focus lies on the efficient power split. Computational delay due to the long prediction horizon is avoided by only recomputing the HLC at specific time steps. In contrast, the LLC is recomputed at every time step for disturbance rejection as it has a lower computational cost.

The paper is structured as follows: Section 2 describes the assumptions and models used for the system dynamics. Section 3 presents the hierarchical control strategy. A simulation study demonstrating the method and the application follows in Section 4. Finally, concluding remarks and further works are given in sections 5 and 6.

2. OFFSHORE HYBRID POWER SYSTEM

The offshore hybrid power system considered in this paper consists of three subsystems: a **gas turbine generator system** (Subsection 2.1), a **wind turbine generator system** (Subsection 2.2), and a **battery system** (Subsection 2.3). These subsystems are only briefly covered with their references and essential simplifications. Readers are advised to refer to the references for the complete mathematical models of each subsystem.

2.1 Gas Turbine Generator Model

The gas turbine generator (GTG) is based on the GAST model (Nagpal et al., 2001) with two simplifications:

- The temperature limit given by load is neglected.
- Friction loss is assumed to be zero.

2.2 Wind Turbine Generator Model

Grunnet et al. (2010) is used for modelling the wind turbine generator (WTG). The WTG model is further simplified by assuming the following (Solberg, 2021):

- The aerodynamics of the wind turbine are approximated with a polynomial.
- Generator torque reference is approximated as a sigmoid function.
- The wind blows perpendicular to the wind turbines.
- The drive train is rigid and without friction.
- The generator torque control is neglected.
- The resulting wind farm is assumed lumped.

2.3 Battery Model

A simple nickel-metal hydride (NiMH) battery model based on Shepherd's model is employed, see Shepherd (1965) and Tremblay et al. (2007). No major assumptions or modifications are made from the references.

2.4 Offshore Hybrid Power System Overview

The resulting OHPS model with noise can be summarised by the system dynamics $\mathbf{f} : \mathbb{R}^{n_\mathbf{x}} \times \mathbb{R}^{n_\mathbf{u}} \times \mathbb{R}^{n_\mathbf{p}} \times \mathbb{R}^{n_\mathbf{w}} \to \mathbb{R}^{n_\mathbf{x}}$ and measurement function $\mathbf{h} : \mathbb{R}^{n_\mathbf{x}} \times \mathbb{R}^{n_\mathbf{u}} \times \mathbb{R}^{n_\mathbf{p}} \to \mathbb{R}^{n_\mathbf{y}}$:

$$\begin{aligned} \mathbf{x_{k+1}} &= \mathbf{f}\left(\mathbf{x_k}, \mathbf{u_k}, \mathbf{p_k}, \mathbf{w_k}\right) \\ \mathbf{y_k} &= \mathbf{h}\left(\mathbf{x_k}, \mathbf{u_k}, \mathbf{p_k}\right) + \mathbf{v_k} \end{aligned} \tag{1}$$

which can be described by the system state vector $\mathbf{x} = [V_{\text{gtg}}, P_{\text{gtg}}, \omega_{\text{wtg}}, M_{\text{wtg,gen}}, \text{SOC}_{\text{bat}}]^{\text{T}} \in \mathbb{R}^{n_\mathbf{x}}$, the system input vector $\mathbf{u} = [T_{\text{gtg}}, \beta_{\text{wtg}}, I_{\text{bat}}]^{\text{T}} \in \mathbb{R}^{n_\mathbf{u}}$, the system parameter vector $\mathbf{p} = [\text{v}_{\text{wind}}]^{\text{T}} \in \mathbb{R}^{n_\mathbf{p}}$, the system output vector $\mathbf{y} = [P_{\text{gtg}}, P_{\text{wtg}}, \text{SOC}_{\text{bat}}, \omega_{\text{wtg}}]^{\text{T}} \in \mathbb{R}^{n_\mathbf{y}}$, process noise vector $\mathbf{w} \in \mathbb{R}^{n_\mathbf{x}}$, and additive measurement noise vector $\mathbf{v} \in \mathbb{R}^{n_\mathbf{y}}$.

Moreover, V_{gtg} [pu] and P_{gtg} [kW] represent the GTG fuel flow and power output, ω_{wtg} [rad s^{-1}] and $M_{\text{wtg,gen}}$ [N m] are the rotational speed of the wind turbine and the WTG generator torque, SOC_{bat} [%] is the battery state of charge (SOC), T_{gtg} [pu] is the GTG throttle, β_{wtg} [deg] is the WTG blade pitch, I_{bat} [A] is the battery current, v_{wind} [m s^{-1}] is the average WTG rotor wind speed, and P_{wtg} [kW] is the WTG power output.

3. HIERARCHICAL CONTROL STRATEGY

The hierarchical strategy consists of two controllers and one observer: an HLC-ENMPC (Subsection 3.1), an LLC-NMPC (Subsection 3.2), and an MHE (Subsection 3.3). Both controllers and the observer formulations are structured according to the standard nonlinear program (NLP) formulation constrained by the system dynamics:

$$\begin{aligned} \min_{\mathbf{x},\mathbf{u}} \quad & \mathbf{J}\left(\mathbf{x_k(t)}, \mathbf{u_k(t)}, \mathbf{p_k(t)}\right) \\ \text{subject to} \quad & \mathbf{x_{k+1}(t)} = \mathbf{f}\left(\mathbf{x_k(t)}, \mathbf{u_k(t)}, \mathbf{p_k(t)}, \mathbf{w_k(t)}\right) \\ & \mathbf{h}_{\text{ineq}}\left(\mathbf{x_k(t)}, \mathbf{u_k(t)}, \mathbf{p_k(t)}\right) \leq \mathbf{0} \\ & \mathbf{g}_{\text{eq}}\left(\mathbf{x_k(t)}, \mathbf{u_k(t)}, \mathbf{p_k(t)}\right) = \mathbf{0} \end{aligned} \tag{2}$$

where $\mathbf{J}(\cdot)$ is the objective function, $\mathbf{x_{k+1}}(\mathbf{t}) = \mathbf{f}(\mathbf{x_k}(\mathbf{t}), \cdots)$ is a vector of equality constraints used to enforce system dynamics for prediction, $\mathbf{h}_{\text{ineq}}(\cdot)$ is a vector of inequality constraints (not to be confused with the measurement function $\mathbf{h}$ from (1)), $\mathbf{g}_{\text{eq}}(\cdot)$ is a vector of equality constraints, $\mathbf{t}$ is current simulation time, and $\mathbf{k} \in \{0, N-1\}$ is the prediction horizon.

Remark 1. The HLC-ENMPC, the LLC-NMPC, and the MHE differ in the objective function $\mathbf{J}(\cdot)$, and the fact that the MPC has to initialise the first decision variable $\mathbf{x}_0$ for continuity as an equality constraint. At the same time, an MHE is not bound to $\mathbf{x}_0$. Additionally, an MHE treats the inputs $\mathbf{u}$ and the outputs $\mathbf{y}$ as parameters to the NLP and optimises the NLP with respect to the system states $\mathbf{x}$ and the process noise $\mathbf{w}$. An MPC optimises for the non-disturbed case where $\mathbf{w} = 0$.

3.1 High-Level Control Formulation

The HLC in this hierarchical control approach consists of an ENMPC. An HLC-ENMPC simplifies the tradeoff between optimal performance and computational cost, as the HLC is only recomputed at specific time steps instead of at every time step to keep the prediction horizon long. The computational cost of the HLC is thus not directly constrained by the system time dynamics as it is not applied at every time step.

To fulfil the total power demand P_{demand} from arbitrarily power consumers while minimising the GHG emissions, the HLC-ENMPC is defined to satisfy the following goal (in decreasing order):

(1) Satisfy the total power demand
(2) Maximise WTG power given the current wind
(3) Minimise GTG power to reduce GHG emissions
(4) Maximise the battery SOC for system flexibility
(5) Minimise actuator effort and additional slack

The high-level objective function $\mathbf{J}_{\text{hlc}}$ that satisfies these objectives is defined as:

$$\begin{aligned}\mathbf{J}_{\text{hlc}} = K_{\text{hlc,gtg}} P_{\text{gtg}} + K_{\text{hlc,wtg}} \left(P_{\text{wtg}} - P_{\text{wtg,max}}\right) - \\ K_{\text{hlc,bat}} \text{SOC}_{\text{bat}} + \mathbf{u}^{\text{T}} K_{\text{hlc,u}} \mathbf{u} + {\mathbf{s}_{\text{hlc}}}^{\text{T}} K_{\text{hlc,s}} \mathbf{s}_{\text{hlc}}\end{aligned}$$

where $K_{\text{hlc,gtg}} \in \mathbb{R}$, $K_{\text{hlc,wtg}} \in \mathbb{R}$, $K_{\text{HLC,bat}} \in \mathbb{R}$, $K_{\text{hlc,u}} \in \mathbb{R}^{n_{\mathbf{u}}} \times \mathbb{R}^{n_{\mathbf{u}}}$, and $K_{\text{hlc,s}} \in \mathbb{R}^{n_{\mathbf{x}}+1} \times \mathbb{R}^{n_{\mathbf{x}}+1}$ are positive scalars/diagonal-matrices. P_{gtg}, P_{wtg}, $P_{\text{wtg,max}}$, and SOC_{bat} are the GTG power, WTG power, WTG max power, and battery state of charge, while $\mathbf{u}$ are the inputs.

The slack variable $\mathbf{s}_{\text{hlc}} \in \mathbb{R}^{n_{\mathbf{x}}+1}$ consists of two parts, one slack variable $\mathbf{s}_{\text{hlc,g}} \in \mathbb{R}$ for the power flow constraint and $\mathbf{s}_{\text{hlc,x}} \in \mathbb{R}^{n_{\mathbf{x}}}$ for converting the constraints on the system states $\mathbf{x}$ into soft constraints. $\mathbf{s}_{\text{hlc,g}}$ is used in the power flow constraint:

$$\mathbf{g}_{\text{hlc}} = P_{\text{gtg}} + P_{\text{wtg}} + P_{\text{bat}} - P_{\text{demand}} + \mathbf{s}_{\text{hlc,g}} \tag{3}$$

which focuses on satisfying the total power demand P_{demand} from the power consumers. A slack variable $\mathbf{s}_{\text{hlc,g}}$ is necessary for infeasibility handling as the OHPS may not satisfy P_{demand} under low average wind conditions and low battery SOC_{bat}, as the GTG power output P_{gtg} is constrained.

In addition to the equality constraint, constraints on the system states $\mathbf{x}$ (formulated as soft constraints for infeasibility handling with $\mathbf{s}_{\text{hlc,x}}$ to handle process noise $\mathbf{w}$), inputs $\mathbf{u}$, the system outputs $\mathbf{y}$, and the slack variables $\mathbf{s}_{\text{hlc}}$ are enforced using inequality constraints to keep the different power systems inside of their nominal operating region as to avoid degradation, see:

$$\mathbf{h}_{\text{hlc,ineq}} = \begin{cases} \mathbf{x}_{\min} \leq \mathbf{x} + \mathbf{s}_{\text{hlc,x}} \leq \inf \\ -\inf \leq \mathbf{x} - \mathbf{s}_{\text{hlc,x}} \leq \mathbf{x}_{\max} \\ \mathbf{u}_{\min} \leq \mathbf{u} \leq \mathbf{u}_{\max} \\ \mathbf{y}_{\min} \leq \mathbf{y} \leq \mathbf{y}_{\max} \\ 0 \leq \mathbf{s}_{\text{hlc}} \leq \inf \end{cases} \tag{4}$$

The resulting NLP for the HLC-ENMPC can be defined as (this form also holds for the LLC):

$$\begin{aligned} \min_{\mathbf{x},\mathbf{u}} \quad & \mathbf{J}_{\text{hlc}}\left(\mathbf{x_k}(\mathbf{t}), \mathbf{u_k}(\mathbf{t}), \mathbf{p_k}(\mathbf{t})\right) \\ \text{subject to} \quad & \mathbf{x_{k+1}}(\mathbf{t}) = \mathbf{f}\left(\mathbf{x_k}(\mathbf{t}), \mathbf{u_k}(\mathbf{t}), \mathbf{p_k}(\mathbf{t}), \mathbf{w_k}(\mathbf{t})\right) \\ & \mathbf{h}_{\text{ineq}}\left(\mathbf{x_k}(\mathbf{t}), \mathbf{u_k}(\mathbf{t}), \mathbf{p_k}(\mathbf{t})\right) \leq \mathbf{0} \\ & \mathbf{g}_{\text{eq}}\left(\mathbf{x_k}(\mathbf{t}), \mathbf{u_k}(\mathbf{t}), \mathbf{p_k}(\mathbf{t})\right) = \mathbf{0} \end{aligned} \tag{5}$$

where $\mathbf{w_k}(\mathbf{t}) = \mathbf{0}$ (*Remark 1*).

3.2 Low-Level Control Formulation

The LLC in this control strategy consists of a conventional tracking NMPC which follows the references computed from the HLC-ENMPC in a receding manner. As opposed to the HLC, the main control objective of the LLC is to (in decreasing order):

(1) Minimise tracking error
(2) Minimise actuator effort and additional slack
(3) Satisfy the total power demand

A tracking NMPC uses a quadratic cost function to track the HLC references. The quadratic low-level cost function $\mathbf{J}_{\text{llc}}$ that fulfils the aforementioned low-level control objective is defined as:

$$\mathbf{J}_{\text{llc}} = {\mathbf{e}_{\mathbf{x}}}^{\text{T}} K_{\text{llc,x}} \mathbf{e}_{\mathbf{x}} + \mathbf{u}^{\text{T}} K_{\text{llc,u}} \mathbf{u} + {\mathbf{s}_{\text{llc}}}^{\text{T}} K_{\text{llc,s}} \mathbf{s}_{\text{llc}}$$

where $K_{\text{llc,x}} \in \mathbb{R}^{n_{\mathbf{x}}} \times \mathbb{R}^{n_{\mathbf{x}}}$, $K_{\text{llc,u}} \in \mathbb{R}^{n_{\mathbf{u}}} \times \mathbb{R}^{n_{\mathbf{u}}}$, and $K_{\text{llc,s}} \in \mathbb{R}^{n_{\mathbf{x}}+1} \times \mathbb{R}^{n_{\mathbf{x}}+1}$ are positive diagonal matrices. $\mathbf{e}_{\mathbf{x}} = (\mathbf{x} - \mathbf{x}_{\text{ref}}) \in \mathbb{R}^{n_{\mathbf{x}}}$ is the error between the system states $\mathbf{x}$ and the HLC system states references $\mathbf{x}_{\text{ref}} \in \mathbb{R}^{n_{\mathbf{x}}}$, $\mathbf{u}$ are the inputs, and $\mathbf{s}_{\text{llc}} \in \mathbb{R}^{n_{\mathbf{x}}+1}$ are slack variables ($\mathbf{s}_{\text{llc}}$ consists similar to $\mathbf{s}_{\text{hlc}}$ of two parts, one variable $\mathbf{s}_{\text{llc,g}} \in \mathbb{R}$ for the power flow constraint and $\mathbf{s}_{\text{llc,x}} \in \mathbb{R}^{n_{\mathbf{x}}}$ for converting the constraints on $\mathbf{x}$ into soft constraints).

Like the HLC, the LLC makes sure that the total power demand P_{demand} is satisfied using (3) with a slack variable $\mathbf{s}_{\text{llc,g}}$ in the event of the arguments in subsection 3.1 and unknown local disturbances, which are not captured in the HLC. Additionally, (3) may be needed due to modelling error if simplifications are made in the HLC.

Remark 2. (3) introduces an implicit constraint in the LLC on the actuator's slew rate to match the power increase and decrease. Without (3), fast systems such as the battery would deliver power faster than, for example,

the WTG, resulting in an under-or overshoot in total delivered power.

Finally, for consistency between the HLC and the LLC: system states $\mathbf{x}$ (formulated as soft constraints using $\mathbf{s}_{\text{llc,x}}$), inputs $\mathbf{u}$, the system outputs $\mathbf{y}$, and the slack variables $\mathbf{s}_{\text{llc}}$ are constrained in the LLC according to (4) to keep the different power systems inside of their standard operating region as to avoid degradation. The resulting NLP for the LLC-NMPC follows (5).

3.3 Observer Formulation

An MHE estimates the system states using past measurements. The main objective of the MHE is to minimise output tracking error and process noise by using a quadratic cost function for estimation.

The quadratic MHE cost function $\mathbf{J}_{\text{mhe}}$ that can estimate optimal system states $\mathbf{x}$ as a balance between the output error and the process noise $\mathbf{w}$ is defined as:

$$\mathbf{J}_{\text{mhe}} = (\mathbf{y} - \mathbf{h}(\mathbf{x}, \mathbf{u}, \mathbf{p}))^{\mathrm{T}} K_{\text{y}} (\mathbf{y} - \mathbf{h}(\mathbf{x}, \mathbf{u}, \mathbf{p})) + \mathbf{w}^{\mathrm{T}} K_{\text{w}} \mathbf{w}$$

where $K_{\text{y}} \in \mathbb{R}^{n_{\mathbf{y}}} \times \mathbb{R}^{n_{\mathbf{y}}}$ and $K_{\text{w}} \in \mathbb{R}^{n_{\mathbf{x}}} \times \mathbb{R}^{n_{\mathbf{x}}}$ are positive diagonal matrices, $\mathbf{x}$ are the system states, $\mathbf{u}$ are the system inputs, $\mathbf{p}$ is the system parameter, $\mathbf{y}$ are the system outputs, $\mathbf{w}$ are the process noise, and $\mathbf{h} : \mathbb{R}^{n_{\mathbf{x}}} \times \mathbb{R}^{n_{\mathbf{u}}} \times \mathbb{R}^{n_{\mathbf{p}}} \to \mathbb{R}^{n_{\mathbf{y}}}$ is the measurement function from (1).

Remark 3. In this case study, the arrival cost is omitted as the estimation performance was satisfactory.

Parameters to the MHE NLP are vectors of past system inputs $\mathbf{u}$, system parameter $\mathbf{p}$, and outputs $\mathbf{y}$ for a predefined window into the past. Thus, the inequality constraints used in the MHE differ from the controllers since $\mathbf{u}$, $\mathbf{p}$, and $\mathbf{y}$ are parameters to the NLP. Additionally, the MHE uses hard constraints for the system states $\mathbf{x}$, and includes the process noise $\mathbf{w}$ in the inequality constraint vector $\mathbf{h}_{\text{ineq,mhe}}$ as it appears as a decision variable in the NLP.

$$\mathbf{h}_{\text{ineq,mhe}} = \begin{cases} \mathbf{x}_{\min} \leq \mathbf{x} \leq \mathbf{x}_{\max} \\ -\inf \leq \mathbf{w} \leq \inf \end{cases} \tag{6}$$

Another difference between the controllers and the MHE is the lack of (3) as an equality constraint. The resulting NLP for the MHE can be defined as:

$$\begin{aligned} \min_{\mathbf{x},\mathbf{w}} \quad & \mathbf{J}_{\text{mhe}}\left(\mathbf{x}_{\mathbf{k}}(\mathbf{t}), \mathbf{u}_{\mathbf{k}}(\mathbf{t}), \mathbf{p}_{\mathbf{k}}(\mathbf{t}), \mathbf{w}_{\mathbf{k}}(\mathbf{t})\right) \\ \text{subject to} \quad & \mathbf{x}_{\mathbf{k+1}}(\mathbf{t}) = \mathbf{f}\left(\mathbf{x}_{\mathbf{k}}(\mathbf{t}), \mathbf{u}_{\mathbf{k}}(\mathbf{t}), \mathbf{p}_{\mathbf{k}}(\mathbf{t}), \mathbf{w}_{\mathbf{k}}(\mathbf{t})\right) \\ & \mathbf{h}_{\text{ineq,mhe}}\left(\mathbf{x}_{\mathbf{k}}(\mathbf{t}), \mathbf{u}_{\mathbf{k}}(\mathbf{t}), \mathbf{p}_{\mathbf{k}}(\mathbf{t})\right) \leq \mathbf{0} \end{aligned} \tag{7}$$

3.4 Hierarchical Control Strategy Overview

The strategy can be summarised by Algorithm 1, which is initialised with initial states $\mathbf{x}_0$ and estimates $\hat{\mathbf{x}}$:

To incorporate feedback into the HLC-ENMPC, the HLC is recomputed at a rate of $\text{t}_{\text{hlc,sampling}}$, where $\text{t}_{\text{hlc,sampling}} < \text{t}_{\text{hlc,prediction}}$. $\text{ENMPC}_{\text{hlc}}(\cdot)$ computes system states references $\mathbf{x}_{\text{ref}}$ given a system states estimates $\hat{\mathbf{x}}$ and system parameter $\mathbf{p}$. The HLC references $\mathbf{x}_{\text{ref}}$ are used in $\text{NMPC}_{\text{llc}}(\cdot)$ together with $\hat{\mathbf{x}}$ and $\mathbf{p}$ to compute optimal local control

Algorithm 1: Hierarchical Control Algorithm

```
// Initialisation
x = x_0;
x̂ = x̂_0;
// Simulation
for (int i = 0; i < n, i++) do
    if (i%t_hlc,sampling == 0) then
        x_ref = ENMPC_hlc(x̂, p);
    u = NMPC_llc(x̂, p, x_ref);
    // Apply u to get next states x given w
    // Measure outputs y from x given v
    x̂ = MHE(u, p, y);
end
```

inputs applied to the OHPS plant, which is disturbed by the process noise $\mathbf{w}$. The **if** condition for the LLC-NMPC, which is computed at a rate of $\text{t}_{\text{llc,sampling}}$ is omitted as it is assumed that $\text{t}_{\text{llc,sampling}}$ is equal to the plant sampling time, and $\text{NMPC}_{\text{llc}}(\cdot)$ is thus applied at every time step.

Similarly, $\text{MHE}(\cdot)$ is applied at every time step and computes the system estimates $\hat{\mathbf{x}}$ given the LLC control inputs $\mathbf{u}$, system parameter $\mathbf{p}$, and noisy measurement $\mathbf{y}$ disturbed by the measurement noise $\mathbf{v}$.

4. SIMULATION AND VALIDATION

This section seeks to validate the performance of the hierarchical control strategy of an OHPS in a simple case study with one power consumer. The simulations are carried out using the simulation environment in Subsection 4.1. Power references from the power consumer for which the controller must satisfy, including the wind dynamics, are briefly covered in Subsection 4.2, while the main results are presented in Subsection 4.3. Lastly, a comparison is made in Subsection 4.4 to illustrate the computational constraints associated with long prediction horizons and why a hierarchical control is required.

4.1 Simulation Environment

The control strategy is simulated on a computer with an Intel(R) Core(TM) i7-9850H CPU @ 2.60 GHz. CasADI (Andersson et al., 2019) is used with multiple shooting (Bock and Plitt, 1984) to formulate the optimal control problems. The optimal control problems are optimised with IPOPT (Wächter and Biegler, 2006) using ma27 (HSL) as the linear solver. The plant model and control model are in this case study identical with the exceptions of process noise ($\mathbf{w} \sim 0$) and normally distributed measurement noise ($\mathbf{v} \sim \mathcal{N}(0, [45, 45, 0.001, 0.001])$), with model parameters adapted from Tremblay et al. (2007) and Solberg (2021). At time $i = 0$, Algorithm 1 is initialised with initial values for the system state $\mathbf{x}_0$ and system estimate $\hat{\mathbf{x}}_0$. These are set equal for simplicity with an value of [0.001, 0.001, 0.9, 0.001, 0.001].

The proposed controller and the plant model are simulated together for 43200 s (12 hours) with a time step of 1 s, corresponding to 43200 iterations. The HLC is recomputed at a rate of $\text{t}_{\text{hlc,sampling}} = 3500$ s with a prediction horizon of 7000 s, while the LLC is recomputed at a rate of $\text{t}_{\text{llc,sampling}} = 1$ s with a prediction horizon of 10 s.

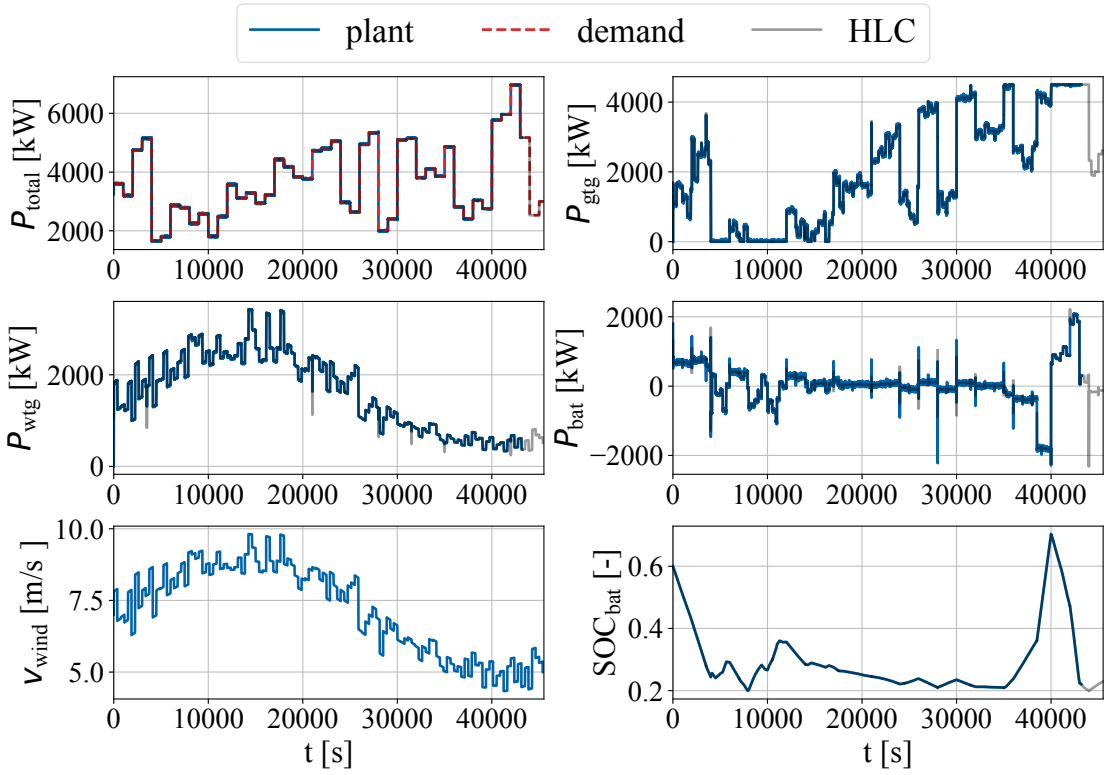

Fig. 3. Time profiles of the closed-loop power response P and battery state of charge SOC_{bat} from applying the hierarchical controller given current wind speed v_{wind}.

Similarly, MHE is recomputed at a rate of $\text{t}_{\text{llc,sampling}} = 1$ s with an estimation horizon of 5 s. It is assumed that the control horizon equals the prediction/estimation horizon. Lastly, tuning constants K_i in the cost function from Subsections 3.1, 3.2, and 3.3 are tuned by hand from simulations according to their importance as defined in their respective Subsections.

4.2 Simulation Variables

In this case study, the wind dynamics are assumed known to illustrate the hierarchical approach's advantage. For simplicity, the wind dynamics is approximated as a noisy sine curve:

$$\text{v}_{\text{wind}} = A_{\text{v}_{\text{wind}}} \sin\left(\frac{1}{f_{\text{v}_{\text{wind}}}}\mathbf{t}\right) + K_{\text{v}_{\text{wind}}} + \mathbf{w}_{\text{v}_{\text{wind}}}$$

where $\mathbf{t}$ is current simulation time, $\text{f}_{\text{v}_{wind}}$ is the frequency of the sine curve, $\text{A}_{\text{v}_{wind}}$ is the amplitude, $\text{K}_{\text{v}_{wind}}$ is the offset, and $\mathbf{w}_{\text{v}_{wind}}$ is white noise that changes values every $T_{s,\mathbf{w}_{\text{v}_{\text{wind}}}}$ s.

Likewise, the total power demand from the power consumer is in this case study modelled using additive noise:

$$P_{\text{demand}} = \mathbf{w}_{\mathbf{P_1}} + \mathbf{w}_{\mathbf{P_2}} \tag{8}$$

where $\mathbf{w}_{\mathbf{P_1}}$ is modelled as a uniform variate random variable that changes values every $T_{s,\mathbf{w}_{\mathbf{P_1}}}$ s, and $\mathbf{w}_{\mathbf{P_2}}$ is additional white noise that changes values every $T_{s,\mathbf{w}_{\mathbf{P_2}}}$ s. Similar to the wind dynamics, the power demand for the whole simulation is assumed known.

The numerical parameters for wind and exogenous power demand forecasts can be found in Table 1.

Table 1. Wind and Exogenous Power Demand Parameters

Symbol	Value	Symbol	Value
$\mathbf{w}_{\text{v}_{\text{wind}}}$	$\mathcal{N}(0,2)$	$\mathbf{w}_{\mathbf{P_1}}$	$\mathcal{U}(2000,6000)$
$K_{\text{v}_{\text{wind}}}$	7	$\mathbf{w}_{\mathbf{P_2}}$	$\mathcal{N}(0,500)$
$A_{\text{v}_{\text{wind}}}, f_{\text{v}_{\text{wind}}}$	2,8500	$T_{s,\mathbf{w}_{\mathbf{P_1}}}$	2000
$T_{s,\mathbf{w}_{\text{v}_{\text{wind}}}}$	375	$T_{s,\mathbf{w}_{\mathbf{P_2}}}$	1000

4.3 Simulation Results

The results from applying the hierarchical controller can be found in Fig. 3. For simplicity, only the power responses P for the GTG, the WTG, and the battery are shown (where $P_{\text{total}} = P_{\text{gtg}} + P_{\text{wtg}} + P_{\text{bat}}$) along with the average WTG rotor wind speed v_{wind} and the battery state of charge SOC_{bat}. These trajectories are computed using the resulting system states $\mathbf{x}$, system inputs $\mathbf{u}$, and system parameter $\mathbf{p}$ from the OHPS plant or the references computed by the HLC-ENMPC. In Fig. 3, the plant response is shown as blue lines, the HLC-ENMPC references are shown as gray lines, and the power demand from the power consumer is shown as stipulated red lines.

Fig. 3 shows that the hierarchical controller distributes and controls the power demand so that the total power demand is always satisfied with the use of the GTG, the WTG, and the battery. The control strategy satisfies total power demand by preemptively charging the battery with the GTG in anticipation of an increase in total power demand and a decrease in v_{wind}. Time of particular interest can be found at t = 40000 s. This time of particular interest is challenging due to $P_{\text{gtg,max}} + P_{\text{wtg,t=40000}} \leq P_{\text{demand,t=40000}}$. Since

Table 2. Comparison results from decreasing the prediction horizons in the HLC-ENMPC.

Prediction Horizon [s]	Average Computational Time [s]	$SOC_{bat,t=\ 40000\ s}$ [%]
7000	19.1	70.4
5000	18.3	55.1
3000	11.4	43.2
500	1	22.4

$P_{gtg,max} + P_{wtg,t=40000} \leq P_{demand,t=40000}$, preemptively charging the battery is important such that $P_{gtg,max} + P_{wtg,t=40000} + P_{bat} = P_{demand,t=40000}$.

In addition to satisfying the total power demand from the power consumer, it can be observed from Fig. 3 that the control strategy satisfies the economic objectives from Subsection 3.1, which is to maximise the WTG power P_{wtg}, while minimising the use of the GTG ($0 \leq P_{gtg}$ during low average wind speed and SOC_{bat} when $P_{wtg} + P_{bat} \leq P_{total,demand}$, otherwise $P_{gtg} \approx 0$).

Remark 4. With a hierarchical approach for an offshore hybrid power system, the GTG usage ($\approx$ 92600 MW when used in a hybrid power system configuration) is lowered by 57.4% compared to the case where the GTG is scaled up to satisfy the power demand alone ($\approx$ 161363 MW).

4.4 Simulation Comparisons

Furthermore, an interesting comparison would be to look at the hierarchical controller for different prediction horizons and see how the controller distributes and controls the power accordingly. Thus, to compare the performance of different prediction horizons, the open-loop power and battery state of charge SOC_{bat} references (the WTG power and the battery power are omitted for simplicity) of the HLC-ENMPC with different prediction horizons ($t_{hlc,prediction}$ = 3000 s, 5000 s, and 7000 s) are plotted in Fig. 4.

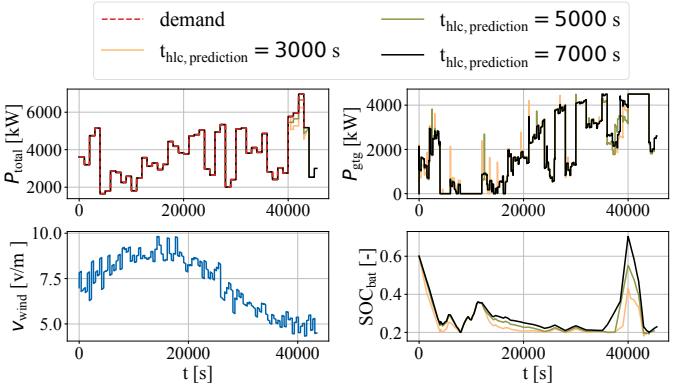

Fig. 4. Time profiles of the open-loop total power P_{total}, GTG power P_{gtg}, and battery state of charge SOC_{bat} references from the HLC-ENMPC with different prediction horizons (decreasing from 7000 s to 3000 s), given current wind speed v_{wind}.

Fig. 4 shows that the reduced horizon controllers ($t_{hlc,prediction}$ = 3000 s and 5000 s) do not satisfy the total power demand. At the time of particular interest (t = 40000 s), the battery state of charge SOC_{bat} is increasing with the prediction horizon. This increase in SOC_{bat} depends on how much time in advance the HLC-ENMPC considers the power demand and the average wind speed at t = 40000 s.

The associated average computational cost of the HLC-ENMPC and the battery SOC at t = 40000 s for different prediction horizons can be found in Table 2. Table 2 shows that all but prediction horizon = 500 s are significantly more than the required computational time for the LLC ($\leq$ 1 s), where the battery SOC is increasing with the prediction horizon.

5. CONCLUDING REMARK

The fast dynamics in the GTG and battery system act as an upper constraint on the computational cost of the actuating controller. If a single ENMPC was used to control the OHPSs, issues due to computational delay would occur as the controller would need $t_{prediction} \leq 7000$ to satisfy the total power demand by utilising wind and power demand forecasts. However, as Table 2 and Fig. 4 illustrate, it is not feasible to only have a single ENMPC versus a hierarchical structure as none of the ENMPCs in Table 2 is wholly solved in 1 s. The maximum prediction horizon corresponding to a sample time of 1 s is 500 s, significantly lower than 7000 s. Hence, this simple case study showcases the advantage of a hierarchical control structure.

A long prediction horizon and intelligent operation of the battery are required in this case study to satisfy the total power demand from the power consumer. This type of operation is required when the case study will be extended to general OEHs, which require a reliable power source in the absence of sufficient GTG power and uncertain renewable generation with energy storage.

However, the results are only valid when the forecasts are perfect regarding the wind and the exogenous power demand. What is gained through a hierarchical controller depends on the forecasts' accuracy, where performance will decrease if the forecasts are unreliable. The impact of uncertain forecasts is, however, out of scope for this work.

In conclusion, a hierarchical control strategy for controlling an OHPS has been proposed to reduce offshore GHG emissions. The advantage of this strategy is an improved scheduling performance due to a long prediction horizon at a relatively low computational cost compared to a single ENMPC with a lower prediction horizon. A simulation study shows how the controller distributes the power such that the total power demand from the power consumer is satisfied at all times, given the wind forecast for that day.

6. FUTURE WORK

This control strategy assumes knowledge of the weather and power demand with their fluctuations. This assump-

tion is not valid in practice, as the weather/power fluctuations are random. Thus, future work should enhance the current controller to handle unknown noise in the weather forecasts and power demand predictions. The final controller must include noise in its formulation to provide a reliable power supply and handling for an eventual OEH application. A way to address noise in an MPC can be robust (Bemporad and Morari, 1999) or stochastic MPC (Mesbah, 2016), depending on the type of noise.

The authors have not considered operational difficulties with offshore wind or batteries. Thus, future work should address the more realistic case, where each system is scaled to a facility at the NCS, and grid stability is considered. Although an offshore hybrid power system does not yet exist, one can take inspiration from the Tampen area in Norway with Hywind Tampen and the Gullfaks and Snorre platforms. Hywind Tampen is a floating offshore wind farm scheduled to provide around 35% of the power demand from Snorre and Gullfaks (Whitfield, 2020).

REFERENCES

J. Andersson, J. Gillis, G. Horn, J. Rawlings, and M. Diehl. CasADi – A software framework for nonlinear optimization and optimal control. *Mathematical Programming Computation*, 11(1):1–36, 2019. doi: 10.1007/s12532-018-0139-4.

A. Bemporad and M. Morari. Robust model predictive control: A survey. In A. Garulli and A. Tesi, editors, *Robustness in identification and control*, pages 207–226, London, 1999. Springer London. ISBN 978-1-84628-538-7.

H. Bock and K. Plitt. A multiple shooting algorithm for direct solution of optimal control problems. *9th IFAC World Congress, Budapest, Hungary*, 17(2):1603–1608, 1984. ISSN 1474-6670. doi: https://doi.org/10.1016/S1474-6670(17)61205-9.

R. Findeisen and F. Allgöwer. Computational delay in nonlinear model predictive control. *IFAC Proceedings Volumes*, 37(1):427–432, 2004. ISSN 1474-6670. doi: https://doi.org/10.1016/S1474-6670(17)38769-4. 7th International Symposium on Advanced Control of Chemical Processes, Hong-Kong, 11-14 January 2004.

J. Gea Bermúdez, R. Bramstoft, M. Koivisto, L. Kitzing, and A. Ramos. Going offshore or not: Where to generate hydrogen in future integrated energy systems? Jun 2021. doi: 10.36227/techrxiv.14806647.v2.

J. Grunnet, M. Soltani, T. Knudsen, M. Kragelund, and T. Bak. Aeolus toolbox for dynamics wind farm model, simulation and control. *European Wind Energy Conference and Exhibition 2010, EWEC 2010*, 4, 01 2010.

T. Hovgaard, K. Edlund, and J. Jørgensen. The potential of economic mpc for power management. *Proceedings of the IEEE Conference on Decision and Control*, pages 7533–7538, 12 2010. doi: 10.1109/CDC.2010.5718175.

HSL. A collection of Fortran codes for large scale scientific computation, http://www.hsl.rl.ac.uk/.

X. Kong, X. Liu, L. Ma, and K. Lee. Hierarchical distributed model predictive control of standalone wind/solar/battery power system. *IEEE Transactions on Systems, Man, and Cybernetics: Systems*, 49(8): 1570–1581, 2019. doi: 10.1109/TSMC.2019.2897646.

P. Kühl, M. Diehl, T. Kraus, J. Schlöder, and H. Bock. A real-time algorithm for moving horizon state and parameter estimation. *Computers & Chemical Engineering*, 35(1):71–83, 2011. ISSN 0098-1354. doi: https://doi.org/10.1016/j.compchemeng.2010.07.012.

T. Marlin and A. Hrymak. Real-time operations optimization of continuous processes. *AIChE Symp Ser CPC V.*, 93, 01 1997.

A. Mesbah. Stochastic model predictive control: An overview and perspectives for future research. *IEEE Control Systems Magazine*, 36(6):30–44, 2016. doi: 10.1109/MCS.2016.2602087.

E. Mikkola, J. Heinonen, M. Kankainen, T. Hekkala, and J. Kurkela. Multi-platform concepts for combining offshore wind energy and fish farming in freezing sea areas: Case study in the gulf of bothnia. In *ASME 2018 37th International Conference on Ocean, Offshore and Arctic Engineering*, volume 6, Oct. 2018. doi: 10.1115/OMAE2018-77677.

T. Morstyn, B. Hredzak, R. Aguilera, and V. Agelidis. Model predictive control for distributed microgrid battery energy storage systems. *IEEE Transactions on Control Systems Technology*, 26(3):1107–1114, 2018. doi: 10.1109/TCST.2017.2699159.

M. Nagpal, A. Moshref, G. Morison, and P. Kundur. Experience with testing and modeling of gas turbines. In *2001 IEEE Power Engineering Society Winter Meeting. Conference Proceedings (Cat. No.01CH37194)*, volume 2, pages 652–656 vol.2, 2001. doi: 10.1109/PESW.2001.916931.

Norwegian Petroleum Directorate. Resource Report, 2019.

J. Rawlings, D. Angeli, and C. Bates. Fundamentals of economic model predictive control. In *2012 IEEE 51st IEEE Conference on Decision and Control (CDC)*, pages 3851–3861, 2012. doi: 10.1109/CDC.2012.6425822.

J. Rawlings, D. Mayne, and M. Diehl. *Model Predictive Control: Theory, Computation, and Design*. Jan. 2017.

C. Shepherd. Design of primary and secondary cells ii. an equation describing battery discharge. *Journal of the Electrochemical Society 112.7*, pages 657 – 667, 1965.

T. Solberg. Nonlinear Model Predictive Control of Offshore Hybrid Power Systems. Trondheim, NTNU ITK, Masterthesis, 2021.

O. Tremblay, L. Dessaint, and A. Dekkiche. A generic battery model for the dynamic simulation of hybrid electric vehicles. *VPPC 2007 - Proceedings of the 2007 IEEE Vehicle Power and Propulsion Conference*, pages 284 – 289, 10 2007. doi: 10.1109/VPPC.2007.4544139.

S. Whitfield. Offshore Wind: The New Frontier in Powering Platforms? *Journal of Petroleum Technology*, 72(01):38–40, 01 2020. ISSN 0149-2136. doi: 10.2118/0120-0038-JPT. URL `https://doi.org/10.2118/0120-0038-JPT`.

A. Wächter and L. Biegler. On the implementation of an interior-point filter line-search algorithm for large-scale nonlinear programming. *Mathematical programming*, 106:25–57, 03 2006. doi: 10.1007/s10107-004-0559-y.

L. Würth, R. Hannemann, and W. Marquardt. A two-layer architecture for economically optimal process control and operation. *Journal of Process Control*, 21(3):311–321, 2011. ISSN 0959-1524. doi: https://doi.org/10.1016/j.jprocont.2010.12.008. Thomas McAvoy Festschrift.